### **RSC Advances**



## PAPER View Article Online View Journal | View Issue



Cite this: RSC Adv., 2024, 14, 6367

# Development of a selective and scalable N1-indazole alkylation†

Jimmy Wang, \*\*D\*\* Aaron Mccreanney, \*\*D\*\* a Amelia Taylor-Young, \*\*‡\* Harriet A. M. Fenton, \*\*D\*\* a Rayyan Miah, \*\*Rebecca A. Johnson, \*\*James Clarke, \*\*Adam Hopkins, \*\*Ricky Jones, \*\*William Waddington, \*\*D\*\* a Steven J. Fussell, \*\*Matthew Badland, \*\*Benjamin Pibworth\*\* and Robert Walton\*\*\*

N1-Alkyl indazoles are a ubiquitous and privileged motif within medicinal chemistry, yet methods to selectively furnish N1-alkyl indazoles with simple alkyl side chains remain sparse. Herein, negative data from high-throughput experimentation (HTE) enabled a confident pivot of resource from continued optimisation to the development of an alternative reaction. This workflow culminated in a methodology for the synthesis of N1-alkyl indazoles. The procedure is highly selective for N1-alkylation, practical, and broad in scope, with no N2-alkyl products detected at completion. Mechanistic understandings were consistent with attributing the high selectivity to thermodynamic control. Additional data-driven process development led to this reaction being safely demonstrated on a 100 g scale, with potential for further scale up. This study highlights pragmatic principles followed to develop a necessitated methodology, suitable for large scale manufacture.

Received 23rd January 2024 Accepted 12th February 2024

DOI: 10.1039/d4ra00598h

rsc.li/rsc-advances

#### Introduction

Regioselective N-functionalisation of ambidentate azoles represents a substantial challenge in organic synthesis and is of particular interest within the pharmaceutical industry due to the high frequency of nitrogen containing heterocycles.<sup>1,2</sup> Indazoles and N1-alkyl indazoles compromise a significant proportion of these heterocycles and are often utilised as indole bioisosteres3 or pharmocophores4,5 (Scheme 1A). Whilst the reaction of indole or pyrrole anions with electrophiles in dipolar aprotic solvents occur predominantly at the lone nitrogen,6 the mesomeric nature of the indazole anion results in comparable conditions leading to highly variable N1: N2 selectivity depending on substrate electronics (Scheme 1B).7,8 Whilst methods exist for the de novo construction of N1-alkyl indazoles,9 regioselective functionalisation of 1H-indazoles with simple, unfunctionalised alkyl groups remains challenging. Available methods are often not applicable to simple alkyl groups, typically relying on activated electrophiles such as oxoniums, 10 α-halo carbonyls, 11,12 and substituted alkenes. 13-18 Recent advances in transition metal catalysis, 19,20 photoredox

catalysis,<sup>21–24</sup> and electrosynthesis<sup>25,26</sup> have provided elegant solutions to help address this issue, however these methodologies can be operationally complex and difficult to scale-up. Herein, the discovery and development of a selective synthesis of unfunctionalised *N*1-alkyl indazoles is described, with

Scheme 1 (A) N1-Alkyl indazoles as bioisosteres³ and pharmacophores⁴.⁵ in medicinal chemistry. (B) Selected example of substrate dependent indazole alkylation selectivity.⁵ (C) Thermodynamically controlled N1-selective indazole alkylation (this work).

<sup>&</sup>lt;sup>a</sup>Pfizer R&D UK Limited, Ramsgate Road, Sandwich, Kent, CT13 9NJ, UK. E-mail: Jimmy.Wang2@pfizer.com; Robert.Walton@pfizer.com

<sup>&</sup>lt;sup>b</sup>Concept Life Sciences, Ramsgate Road, Sandwich, Kent, CT13 9NJ, UK

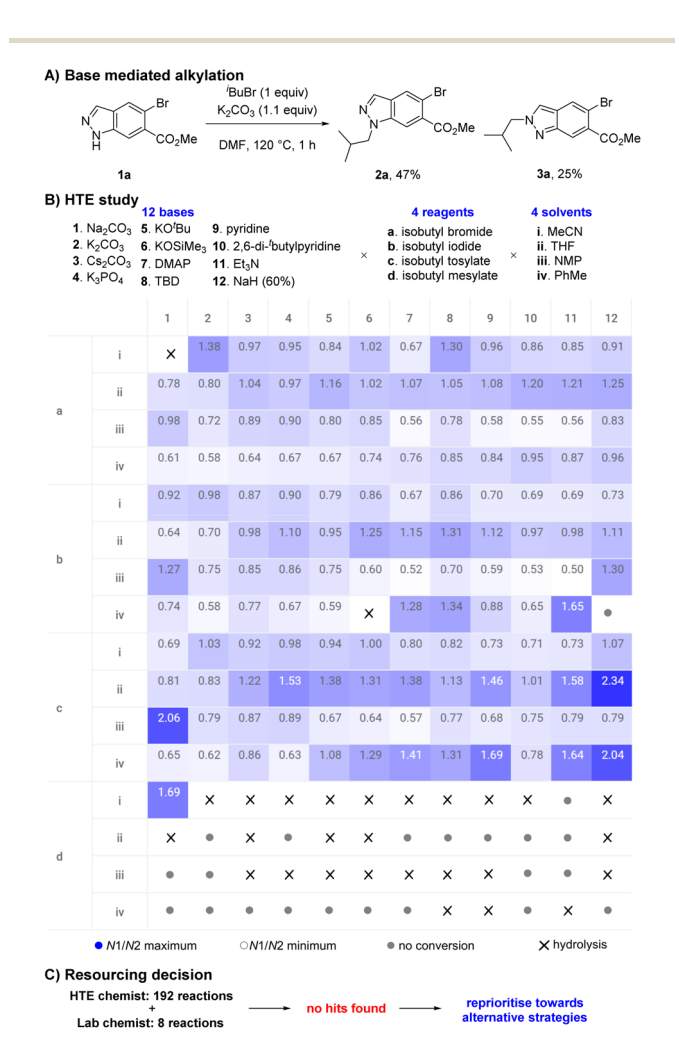
<sup>†</sup> Electronic supplementary information (ESI) available: Experimental details, including procedures, additional optimisation data, compound characterisation, process safety data, NMR spectra. See DOI: https://doi.org/10.1039/d4ra00598h

<sup>‡</sup> AM and ATY contributed equally to this work.

selectivity dictated by thermodynamics and a procedure suitable for large scale manufacture (Scheme 1C).

#### Results and discussion

During an internal development program, a selective and scalable<sup>27</sup> transformation of indazole **1a** to its N1-isobutyl variant **2a** was required. This indazole featured an aryl-bromide sensitive to transition metal chemistry, a methyl ester prone to hydrolysis, no steric bias at C3 or C7, and was available to us on kilogram scale. Typical base mediated  $S_N2$  conditions to facilitate indazole **1a** reacting with isobutyl bromide ( $K_2CO_3$ , DMF, 120 °C) resulted in full conversion but gave a 58:42 mixture of N1:N2 isomers **2a** and **3a**. Chromatography was required to separate and isolate desired product **2a** in 47% yield; undesired isomer **3a** was also obtained in 25% yield (Scheme 2A). The direct alkylation of **1a** with an isobutyl group was the most attractive and synthetically straightforward method available to



Scheme 2 (A) Indazole alkylation using standard alkylation conditions. Crude 2a:3a ratio was 58:42 by LCMS (225 nm). (B) HTE study and selectivity results in a heat map. Standard conditions stirred 15 mg 1a, 1.1 equiv. base, 1 equiv. reagent, and  $300~\mu$ L solvent at  $50~^{\circ}$ C for 16~h. DMAP = 4-dimethylaminopyridine; TBD = triazabicyclodecene. (C) Workflow followed leading to reprioritisation of resourcing.

access the desired product 2a, however the low selectivity displayed was a concern.

High-throughput experimentation (HTE) utilises technological advancements in automation and robotics to significantly accelerate the exploration of chemical space by executing numerous small-scale experiments in parallel.28-30 HTE has transformed the field of synthetic organic chemistry, rapidly increasing the rate of reaction discovery, 31,32 reaction optimisation,33 and reaction scope evaluation.34,35 We initially leveraged our HTE capabilities to explore the influence of discrete variables to increase the selectivity in favour of desired product 2a. A study to explore diverse chemical space was designed involving 12 bases, 4 reagents, and 4 solvents, then executed using automated technologies and analysed with data visualisation techniques (Scheme 2B). Our results suggested the system could be tuned to favour either 2a or 3a in a limited fashion by selecting an appropriate combination of base, reagent, and solvent. However, the highest ratio of 2a:3a remained a moderate 2.34 (70:30) (NaH (60%), isobutyl tosylate, THF) and was insufficient to offer a useful preparative method.

Alongside the HTE study, data from 8 experiments from a lab chemist were also obtained, suggesting our HTE capabilities provided an approximate 24-fold time save (Scheme 2C). Unfortunately, these combined learnings failed to reveal suitable hits within the explored chemical space. We believed further optimisation would be highly unlikely to produce desired results and a decision to reprioritise resources was taken.

One strategy we explored focused on utilising isobutyraldehyde to introduce the isobutyl group through a formal reductive amination process. Reacting indazole 1a under standard reductive amination conditions36 resulted in negligible conversion and no detectable iminium formation (Table 1, entry 1). However, a two-step process of initial enamine condensation and subsequent hydrogenation resulted in success. Crucially, exclusive N1 selectivity was observed during the initial enamine formation, with the major side product found to be aminal pseudo-dimer 5a. To maximise conversion to 4a and minimise formation of 5a, an excess of aldehyde and effective water removal was essential. Dean-Stark conditions were highly effective compared to either a typical reflux or use of molecular sieves (Table 1, entries 2-4). Cooling the reaction below reflux resulted in some reversion of 4a to 5a, hence a quench with triethylamine was introduced at reflux to maintain high selectivity for 4a (Table 1, entries 5-7). Metal catalysed hydrogenations are highly scalable and 5% Pt/C was discovered to be the most active and efficient catalyst, providing full conversion whilst minimising dehalogenation (see ESI† for full details). Enamine 4a could be isolated crude and reacted further under an atmosphere of H<sub>2</sub> at 40 psi and 30 °C with 5% Pt/C to afford 2a in high conversion whilst minimising overreduction of the aryl bromide. The transformation of indazole 1a to desired product 2a was achieved in two steps and a single purification in 76% yield, with no detectable N2 isomer produced (Table 1, entry 7).

Table 1 Selected optimisation (enamine synthesis)

Entry	Variation from above	Conversion (ratio 4a:5a)
1	Na(OAc)₃BH, 1,2-dichloroethane	n.d.
2	4 Å MS, 24 h	97% (52:48)
3	None	95% (82:18)
4	Dean-Stark, sampled at reflux	>99% (>99:1)
5	Isobutyraldehyde (2 equiv.), Dean-Stark, sampled at reflux	95% (90:10)
6	Dean-Stark, sampled at rt	97% (96:4)
7	Dean-Stark, then Et <sub>3</sub> N (0.25 equiv.), sampled at rt	>99% (>99:1) 76% yield <sup>a</sup>

a isolated yield of 2a after hydrogenation of 4a (H<sub>2</sub> (40 psi), 5% Pt/C (0.013 equiv.), PhMe, 30 °C), over two steps. MS = molecular sieves.

Following the development of a selective and robust transformation of indazole 1a to alkylated product 2a, the substrate scope of this reaction was explored to understand both its potential and limitations (Scheme 3). Using isobutyraldehyde as the alkylating partner our conditions were highly robust to changes in indazole electronics. 3-, 4-, 5-, and 6-carboxylate indazoles were all functionalised selectively at the N1 position (2c-f), whilst 7-carboxylate indazole remained unreactive (2g). As 7-bromoindazole reacted to form 2h in 27% yield, it is plausible the lack of reactivity with 7-carboxylate indazole was due to steric effects. In addition to the electron withdrawing esters and aryl bromides, the reaction also proceeded well with electronically neutral indazole (2b), fluorinated indazoles (2i-j), and electron rich methoxy (2k) and alkyl (2l) substituted indazoles.

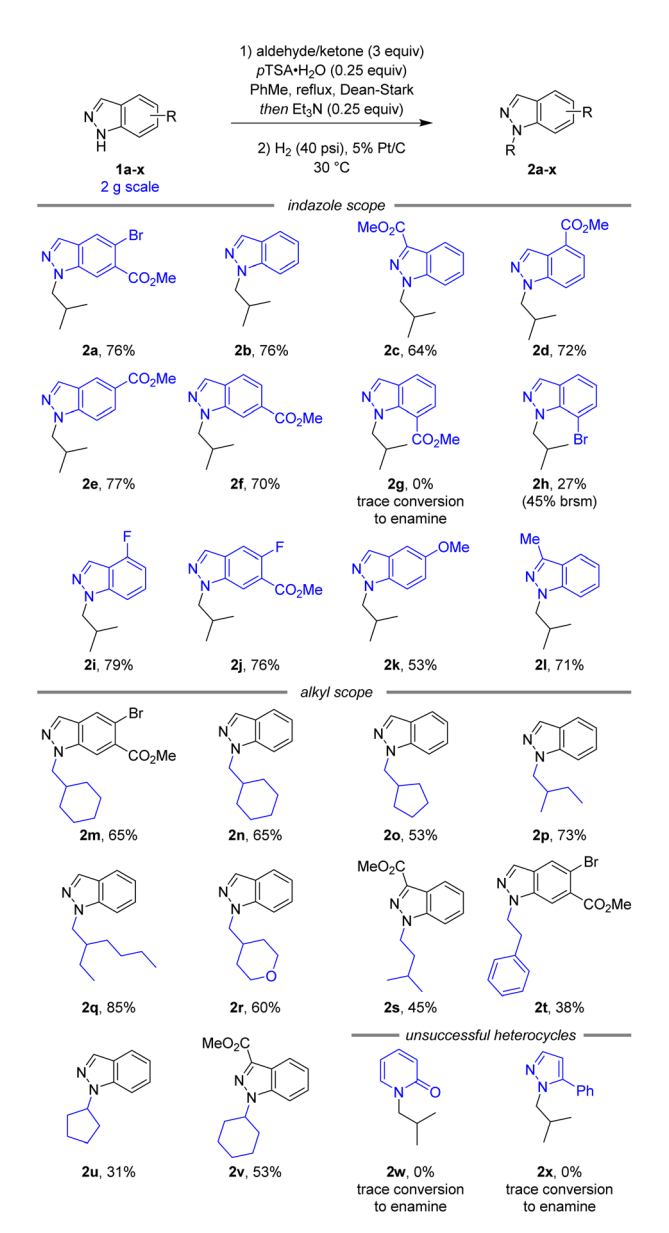
A variety of simple alkyl reaction partners also reacted smoothly, maintaining N1 selectivity and high yields. Both cyclic (2m-o) and linear (2p-q) secondary aldehydes afforded the corresponding N1-alkyl-indazoles in good yields. An electronic variation in tetrahydro-2H-pyran-4-carbaldehyde continued to afford the corresponding product (2r) in good yield and selectivity. Reactions with primary aldehydes isovaleraldehyde (2s) and phenylacetaldehyde (2t) were also successful, although the products were obtained in slightly lower yield due to the decreased stability of the intermediate enamine. Additionally, this reaction was successful with simple ketones (2u,v), despite the increased steric hindrance and decreased reactivity of the alkylation reagent. Unfortunately, attempts to extend this methodology beyond indazoles to 2pyridone (2w) and pyrazole (2x) heterocycles were unsuccessful.

Further investigations were enacted to understand the formation of aminal pseudodimer **5a** and the high preference for enamine **4a**. *N*1-selective indazole functionalisations often possess an element of reversibility, with selectivity attributed to thermodynamic control. Time-course data was gathered to explore this hypothesis. Potential intermediates including the

*N*1 enamine **4a**, *N*2 enamine **6a**, *N*1,*N*1-aminal **5a**, and *N*1-*N*2 aminal pseudodimers **7a** were independently synthesised, isolated, and fully characterised.

Monitoring this reaction by LCMS with biphenyl as internal standard provided valuable insights into the reaction composition during its progression. In the standard reaction, large quantities of aminal pseudo-dimers 5a and 7a form at the start of the reaction, decreasing as the reaction progresses (Scheme 4A(i)). Whilst the N1,N2-aminal 7a depleted rapidly, the N1,N1aminal 5a persists for longer, suggesting it is the more stable of the two. As discovered during reaction optimisation, continued heating leads to degradation of product 4a and reformation of aminal 5a. Commencing the standard reaction with 0.5 equiv. isobutyraldehyde resulted in a plateau containing a near equal mixture of starting material 1a, enamine product 4a, and 5a. An additional charge of 2.5 equiv. isobutyraldehyde resulted in a brief increase in 7a, before consumption of 1a, 5a, and 7a to form product 2a (Scheme 4A(ii)). Heating chromatographically purified 4a with  $pTSA \cdot H_2O$  in the absence of isobutyraldehyde resulted in noticeable increase of indazole 1a, aminal 5a, and small quantities of aminal 7a, whereas no reaction was observed in absence of  $pTSA \cdot H_2O$  (Scheme 4A(iii)).

Our proposed mechanism involves reversible equilibrium between all species involved, including indazole  ${\bf 1a}$ , aminals  ${\bf 5a}$  and  ${\bf 7a}$ , and enamine  ${\bf 4a}$ . Indazole  ${\bf 1a}$  can condense rapidly with isobutyraldehyde to form either  ${\bf 5a}$  or  ${\bf 7a}$ . Whilst  ${\bf 7a}$  appears unstable and likely reacts to form both  ${\bf 4a}$  and  ${\bf 1a}$ ,  ${\bf 5a}$  is evidently thermodynamically favoured, reacting with excess aldehyde to produce enamine  ${\bf 4a}$  (Scheme  ${\bf 4B}$ ). The tendency of  ${\bf 4a}$  to reform  ${\bf 5a}$  can be attributed to a reduction in aldehyde excess owing to its inherent volatility (bp =  ${\bf 63}$  °C) and instability towards adventitious oxygen. This was further supported by observations of decreased conversion to  ${\bf 4a}$  in reactions with inefficient condensers. These investigations were consistent with attributing the high regioselectivity to thermodynamic control and

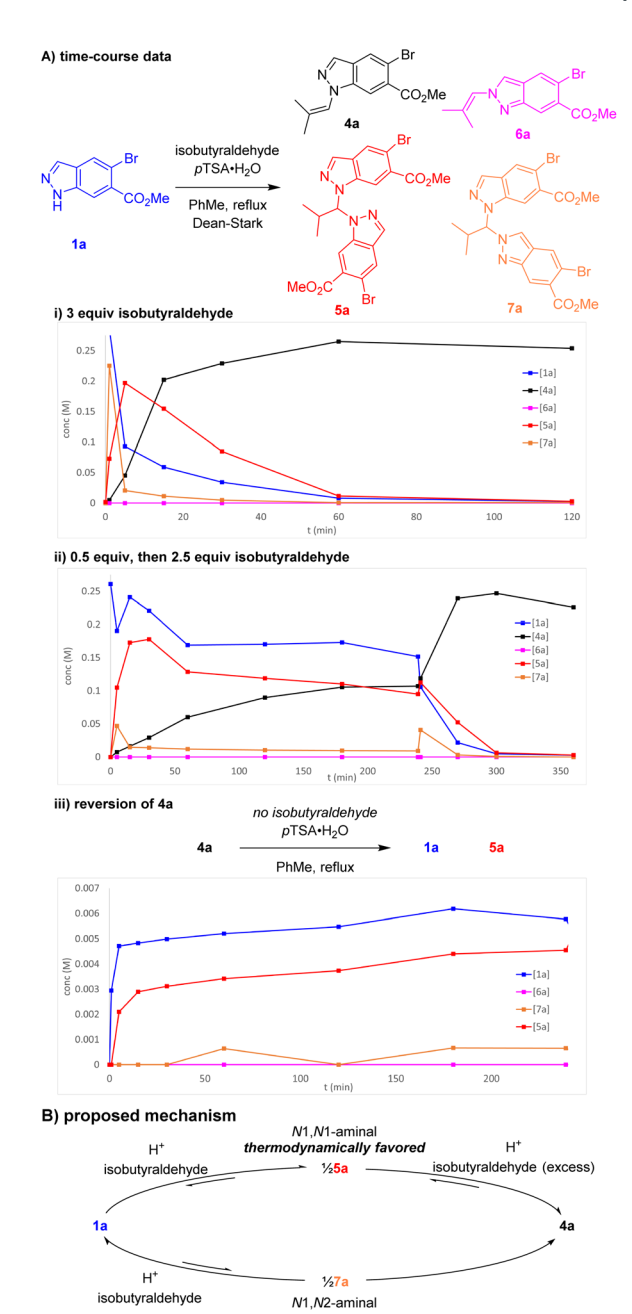


**Scheme 3** Reaction scope and limitations.<sup>a</sup> <sup>a</sup>All yields are isolated yields over two steps. brsm = based on recovered starting material.

highlighted the importance of the  $Et_3N$  addition to avoid reversion of product  ${\bf 4a}$  to the aminal  ${\bf 5a}$ .

From the outset of this development program, we aimed to produce N1-alkyl indazole 2a on a multi-kilogram scale. Despite the streamlined telescope procedure employed, undesirable processes such as use of MgSO<sub>4</sub> as desiccant, multiple distillations to dryness, and chromatographic purification remained, resulting in a high PMI (process mass intensity)<sup>37</sup> of >500 and necessitated additional process development (Fig. 1A). In addition, the nitrogen–nitrogen bond within the indazole raised process safety concerns and additional studies were required to de-risk potential issues upon scale-up.

The initial workup involved washes with  $H_2O$ , 1 M  $HCl_{(aq)}$  and saturated brine, before drying with MgSO<sub>4</sub>, filtration, evaporation to dryness, and redissolution in PhMe. Additional



Scheme 4 (A) Key time-course data of reaction of 1a and isobutyraldehyde. Concentrations determined by LCMS with biphenyl internal standard. (B) Proposed reaction mechanism for enamine condensation.

experimentation revealed removal of the  $HCl_{(aq)}$  wash and replacing the  $MgSO_4$  desiccant with a controlled azeotropic distillation resulted in negligible impact to reaction yield or purity (Fig. 1B(i)). Although no instability of enamine towards the  $HCl_{(aq)}$  wash was observed, its removal further derisked potential acid catalysed enamine hydrolysis. These modifications enabled both a reduction in PMI and unit operations, increasing throughput and resulting in a more streamlined process for manufacture.

Conditions to crystallise 2a were sought to avoid chromatographic purification and significantly reduce PMI (Fig. 1B(ii)).

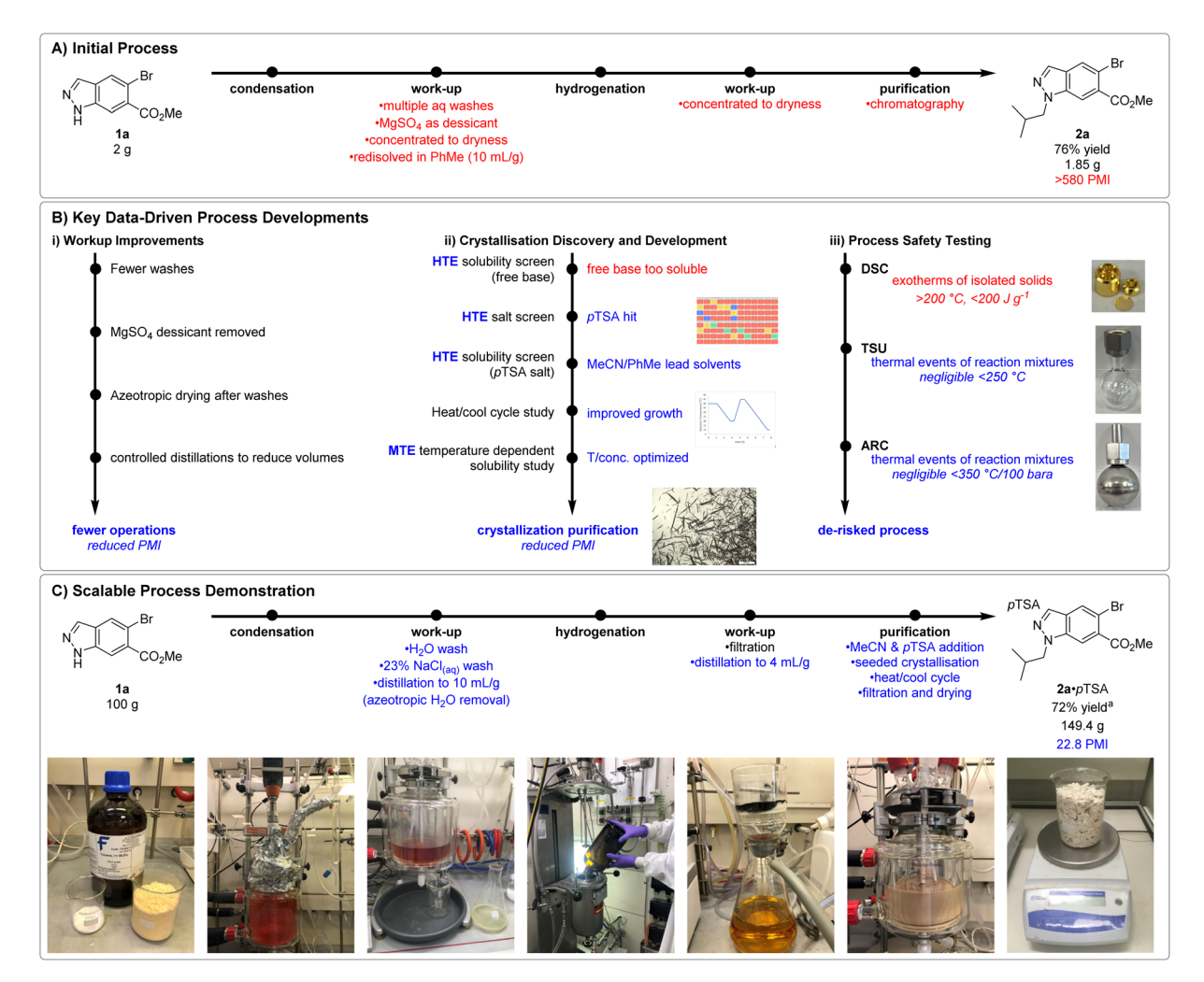


Fig. 1 (A) Initial process followed for reaction scope. (B) Key process improvements including crystallisation discovery and development, workup improvements, and process safety testing. (C) Scalable process demonstration on 100 g scale. From left to right: starting materials and solvent; reaction in 2 L jacketed vessel; distillation and workup in 5 L jacketed vessel; charging of hydrogenation reaction; removal of hydrogenation catalyst by filtration over arbocel; crystallisation of 2a as the pTSA salt; isolated final product. <sup>a</sup>Final product contained 1.25 equiv. pTSA by NMR. PMI = Process mass intensity. DSC = differential scanning calorimetry. TSU = thermal screening unit. ARC = accelerated rate calorimetry.

We once again leveraged our HTE resources to swiftly realise freebase 2a possessed high (>90 mg mL<sup>-1</sup>) solubility in a diverse set of 22 (binary)-solvent systems and would likely require isolation as a salt. Subsequently a HTE salt screen was performed, studying the mixture observed upon combining 2a with 24 acids in 4 process relevant solvents (MeCN, IPA, EtOAc, and PhMe). 9 conditions were found to produce slurries suitable for filtration, notably pTSA·H<sub>2</sub>O in the reaction solvent PhMe, and pTSA·H<sub>2</sub>O in MeCN. Gram scale synthesis and isolation of  $2a \cdot p$ TSA provided material to support further crystallisation development. Additional HTE solubility screens with 2a·pTSA in 46 (binary)-solvent systems highlighted the ability of MeCN to modulate the solubility of the  $2a \cdot p$ TSA salt in PhMe. Solvent systems containing <30% MeCN in PhMe provided the steepest solubility gradient, allowing for good solubility at high temperatures whilst maximising recovery at low temperatures. The initial slurries were typically slow to filter and optical microscopy revealed many fine particles. A heat-cool cycle was

found to significantly improve the particle size distribution and filtration speed via Ostwald ripening.38 Lastly, temperature dependent solubility curves of 2a·pTSA in MeCN: PhMe mixtures were studied in a medium-throughput fashion using the Crystal16 benchtop crystallisation system. These studies led to a procedure in which a solution of crude 2a in PhMe taken directly after hydrogenation and catalyst removal would be concentrated to 6.7 mL  $g^{-1}$  (vs. initial 1a) and diluted with MeCN (2.2 mL  $g^{-1}$  vs. initial 1a). Addition of pTSA·H<sub>2</sub>O and  $2a \cdot p$ TSA seed (0.01 equiv.) at 40 °C, followed by aging, heat-cool cycling, granulation, and collection by filtration at 10 °C yielded pure  $2a \cdot p$ TSA in 76% yield on 7.5 g scale.

Compounds containing functional groups with a nitrogennitrogen bond are known for their potential to release significant amounts of energy as they decompose, 39 presenting the potential for process safety issues upon scale-up. To minimise process risks, it was essential to understand the thermal characteristics of isolated materials and reaction mixtures

generated. These thermal characteristics were assessed using Differential Scanning Calorimetry (DSC), Thermal Screening Unit (TSU) and Accelerating Rate Calorimetry (ARC) for the reaction with 100 g 1a (Fig. 1B(iii)). Isolated solids of 1a, 4a, 2a and 2a·pTSA all displayed significant exotherms formation at temperatures above 200 °C in the initial DSC analysis, and exotherms and gas formation in subsequent ARC analysis. In all cases, the adiabatic temperature rise was found to be >200 °C, suggesting potential process risks relating to the thermal stability of the reaction mixtures. Fortunately, further thermal stability testing by TSU and ARC of the pre- and post-reaction mixtures for the enamine condensation to form 4a displayed no significant thermal events. Additional TSU testing of the preand post-reaction mixtures for the hydrogenation of 4a to 2a displayed some minor thermal events which were not associated with gas formation and were deemed negligible in the context of this process.

These improvements to work-up, purification, and process safety understanding enabled confidence in proceeding with a 100 g scale demonstration of an indazole alkylation. Our combined data-driven learnings culminated in a reproducible process for the isolation of  $2a \cdot p$ TSA as a crystalline solid in 72% yield (149.4 g product) over two steps and a significant reduced PMI of 22.8, down from >500 (Fig. 1C).

#### Conclusions

In summary, we have described the discovery and development of a thermodynamically driven N1-selective indazole alkylation. Throughout this study, we accelerated development by leveraging both positive and negative data from HTE. A broad scope was demonstrated, and mechanistic investigations corroborated our hypothesis that the high observed selectivity of this reaction was due to thermodynamic control. Process safety understanding and additional process optimisation lead to the successful completion of this reaction on a 100 g scale ready for multi-kilogram production in a pilot plant. During the preparation of this manuscript, the largest single batch used 321.6 kg of 1a to produce 408.4 kg of 2a·pTSA (67% yield, hydrogenation split into two batches); overall, >1 MT of  $2a \cdot p$ TSA has been manufactured with this process. We anticipate the core principles presented in this article will see further applications across both academia and industry.

#### Author contributions

Conceptualization and supervision: RW, JW. Project administration and resources: RW. Investigation: JW, AM, ATY, HAMF, RM, RAJ, JC, AH, RJ, WSW, SJF, MB, BP. Visualisation and writing – original draft: JW, ATY, HAMF, JC, RAJ. Writing – review & editing: JW, JC, SJF, RW.

#### Conflicts of interest

There are no conflicts to declare.

#### Acknowledgements

We thank numerous colleagues within Pfizer and Array Bio-Pharma, as well as our external collaborators at CROs and CMDOs for their helpful ideas, discussions, and contributions to this research program. We thank Donald A. Clark, Ryan Osborne, and Shams T. A. Islam for assistance with analytical data collection. We thank Ian Moses, Philip Peach, and Phillip Greenwood for additional experimental support. We thank Michael Hawksworth, Caroline Chapman, and Heather Ingram for assistance with process safety data collection.

#### Notes and references

- 1 E. Vitaku, D. T. Smith and J. T. Njardarson, *J. Med. Chem.*, 2014, 57, 10257–10274.
- 2 R. D. Taylor, M. MacCoss and A. D. Lawson, J. Med. Chem., 2014, 57, 5845–5859.
- 3 P. Fludzinski, D. A. Evrard, W. E. Bloomquist, W. B. Lacefield, W. Pfeifer, N. D. Jones, J. B. Deeter and M. L. Cohen, *J. Med. Chem.*, 1987, 30, 1535–1537.
- 4 WO Pat., WO2004078116A2, 2004.
- 5 P. A. Quane, G. G. Graham and J. B. Ziegler, *Inflammopharmacology*, 1998, **6**, 95–107.
- 6 H. Heaney and S. V. Ley, J. Chem. Soc., Perkin Trans. 1, 1973, 499–500.
- 7 R. M. Alam and J. J. Keating, *Beilstein J. Org. Chem.*, 2021, 17, 1939–1951.
- 8 H. He, J. Yan, J. Jin, Z. Yan, Q. Yan, W. Wang, H. Jiang, H. Wang and F. Chen, *Chem. Commun.*, 2022, **58**, 6429–6432.
- N. Cankařová, J. Hlaváč and V. Krchňák, Org. Prep. Proced. Int., 2010, 42, 433-465.
- 10 D. J. Slade, N. F. Pelz, W. Bodnar, J. W. Lampe and P. S. Watson, J. Org. Chem., 2009, 74, 6331–6334.
- 11 K. W. Hunt, D. A. Moreno, N. Suiter, C. T. Clark and G. Kim, *Org. Lett.*, 2009, **11**, 5054–5057.
- 12 M. N. Vander Wal, A. K. Dilger and D. W. C. MacMillan, *Chem. Sci.*, 2013, 4, 3075–3079.
- 13 J. Moran, P. Dornan and A. M. Beauchemin, *Org. Lett.*, 2007, 9, 3893–3896.
- 14 S. W. Kim, T. T. Schempp, J. R. Zbieg, C. E. Stivala and M. J. Krische, *Angew Chem. Int. Ed. Engl.*, 2019, 58, 7762– 7766.
- 15 W. S. Jiang, D. W. Ji, W. S. Zhang, G. Zhang, X. T. Min, Y. C. Hu, X. L. Jiang and Q. A. Chen, *Angew Chem. Int. Ed. Engl.*, 2021, 60, 8321–8328.
- 16 Q. C. Xue, J. Xie, P. Xu, K. D. Hu, Y. X. Cheng and C. J. Zhu, ACS Catal., 2013, 3, 1365–1368.
- 17 A. M. Haydl, K. Xu and B. Breit, *Angew Chem. Int. Ed. Engl.*, 2015, **54**, 7149–7153.
- 18 J. Y. Yang, Y. F. Bao, H. Y. Zhou, T. Y. Li, N. N. Li and Z. Li, *Synthesis*, 2016, **48**, 1139–1146.
- 19 B. Górski, A.-L. Barthelemy, J. J. Douglas, F. Juliá and D. Leonori, *Nat. Catal.*, 2021, 4, 623–630.
- 20 X. Y. Lv, R. Abrams and R. Martin, *Angew Chem. Int. Ed. Engl.*, 2023, **62**, e202217386.

- 21 Y. Liang, X. Zhang and D. W. C. MacMillan, *Nature*, 2018, 559, 83–88.
- 22 N. W. Dow, A. Cabre and D. W. C. MacMillan, *Chem*, 2021, 7, 1827–1842.
- 23 V. T. Nguyen, V. D. Nguyen, G. C. Haug, N. T. H. Vuong, H. T. Dang, H. D. Arman and O. V. Larionov, *Angew Chem. Int. Ed. Engl.*, 2020, 59, 7921–7927.
- 24 Y. Ge, Y. Shao, S. Wu, P. Liu, J. Li, H. Qin, Y. Zhang, X.-s. Xue and Y. Chen, *ACS Catal.*, 2023, **13**, 3749–3756.
- 25 L. Sun, X. Zhang, C. Wang, H. Teng, J. Ma, Z. Li, H. Chen and H. Jiang, *Green Chem.*, 2019, **21**, 2732–2738.
- 26 J. W. Wu, Y. Zhou, Y. C. Zhou, C. W. Chiang and A. W. Lei, *ACS Catal.*, 2017, 7, 8320–8323.
- 27 M. Butters, D. Catterick, A. Craig, A. Curzons, D. Dale, A. Gillmore, S. P. Green, I. Marziano, J. P. Sherlock and W. White, *Chem. Rev.*, 2006, **106**, 3002–3027.
- 28 J. R. Schmink, A. Bellomo and S. Berritt, *Aldrichimica Acta*, 2013, **46**, 71–80.
- 29 S. M. Mennen, C. Alhambra, C. L. Allen, M. Barberis, S. Berritt, T. A. Brandt, A. D. Campbell, J. Castanon, A. H. Cherney, M. Christensen, D. B. Damon, J. E. de Diego, S. Garcia-Cerrada, P. Garcia-Losada, R. Haro, J. Janey, D. C. Leitch, L. Li, F. F. Liu, P. C. Lobben, D. W. C. MacMillan, J. Magano, E. McInturff, S. Monfette,

- R. J. Post, D. Schultz, B. J. Sitter, J. M. Stevens, J. I. Strambeanu, J. Twilton, K. Wang and M. A. Zajac, *Org. Process Res. Dev.*, 2019, 23, 1213–1242.
- 30 M. Shevlin, ACS Med. Chem. Lett., 2017, 8, 601-607.
- 31 A. McNally, C. K. Prier and D. W. MacMillan, *Science*, 2011, 334, 1114–1117.
- 32 K. D. Collins, T. Gensch and F. Glorius, *Nat. Chem.*, 2014, 6, 859–871.
- 33 S. M. Preshlock, B. Ghaffari, P. E. Maligres, S. W. Krska, R. E. Maleczka Jr and M. R. Smith 3rd, *J. Am. Chem. Soc.*, 2013, 135, 7572–7582.
- 34 C. C. Wagen, S. E. McMinn, E. E. Kwan and E. N. Jacobsen, *Nature*, 2022, **610**, 680–686.
- 35 K. Kang, N. L. Loud, T. A. DiBenedetto and D. J. Weix, *J. Am. Chem. Soc.*, 2021, **143**, 21484–21491.
- 36 A. F. Abdel-Magid, K. G. Carson, B. D. Harris, C. A. Maryanoff and R. D. Shah, J. Org. Chem., 1996, 61, 3849–3862.
- 37 C. Jimenez-Gonzalez, C. S. Ponder, Q. B. Broxterman and J. B. Manley, *Org. Process Res. Dev.*, 2011, **15**, 912–917.
- 38 I. M. Lifshitz and V. V. Slyozov, *J. Phys. Chem. Solids*, 1961, **19**, 35–50.
- 39 Bretherick's Handbook of Reactive Chemical Hazards, ed. P. G. Urben, Elsevier, 8th edn, 2017.